EPR study of carbon and silicon related defects in carbon-rich hydrogenated amorphous silicon-carbon films

E. N. Kalabukhova,[1] S. N. Lukin,[1] D. V. Savchenko,[1] B. D. Shanina,[1] A. V. Vasin,[1] V. S. Lysenko,[1] A. N. Nazarov,[1] A. V. Rusavsky,[1] J. Hoentsch,[2] and Y. Koshka[3]

[1]*V. E. Lashkaryov Institute of Semiconductor Physics, NASU, Prospect Nauki 45, 03028 Kiev, Ukraine*

[2]*Faculty of Physics and Earth Sciences, Institute of Experimental Physics II, Leipzig University, Linnéstrasse 5, D-04103 Leipzig, Germany*

[3]*Department of Electrical and Computer Engineering, Mississippi State University, P.O. Box 9571, Mississippi 39762, USA*

(Received 22 June 2009; revised manuscript received 8 February 2010; published 22 April 2010)

Three paramagnetic defects were revealed in amorphous hydrogenated carbon-rich silicon-carbon alloy films (a-$Si_{0.3}C_{0.7}$:H). Two of them were attributed to silicon (Si) dangling bonds (Si DBs) and carbon-related defects (CRDs). The third defect, based on its g-value and linewidth, was tentatively attributed to a bulk Si DB defect bonded with nitrogen atoms in Si-N_2Si configuration. The effect of thermal vacuum annealing on the properties of the a-$Si_{0.3}C_{0.7}$:H films was studied in the temperature range of $T_{ann}=400-950$ °C. A strong increase in CRD concentration was observed in high temperature annealed a-$Si_{0.3}C_{0.7}$:H films, which was explained by hydrogen effusion process occurred at T_{ann} above 400 °C. The increase in the concentration of the CRDs is accompanied by the exchange narrowing of its electron paramagnetic resonance (EPR) linewidth due to the formation of carbon clusters having ferromagnetic ordering. The temperature dependent g-factor anisotropies observed at Q-band and D-band frequencies for the CRD signal in the samples annealed at high temperature (950 °C) were explained by the presence of graphitelike sp^2-coordinated carbon clusters and demagnetization field (shape-dependent anisotropy term). The demagnetizing field $B_{dem}=-4\pi M_s$, where M_s is the sample magnetization, was found to be equal to 0.44 mT at 37 GHz and 1.1 mT at 140 GHz. Analysis of the temperature dependences of the integral intensities of the SiDB and CRD EPR signals has shown that they do not obey the Curie-Weiss law, and their spin systems exhibit superparamagnetic and ferromagnetic properties, respectively.

DOI: 10.1103/PhysRevB.81.155319 PACS number(s): 73.61.Jc

I. INTRODUCTION

Silicon-carbon amorphous hydrogenated alloys (a-$Si_{1-x}C_x$:H) have attracted great interest since they can be used for production of a large variety of thin film materials with tuneable electrical, optical, and light emitting properties.[1–10] It was shown that the variation of the optical band gap from 1.4 to 3.0 eV as well as the photoluminescence color from red to blue can be modulated by carbon and hydrogen incorporation in these materials.[1–5] However, the microstructure, the nature of defects and their relation to the contents of carbon, hydrogen and annealing treatment are still the major research subjects in semiconductor physics of a-$Si_{1-x}C_x$:H, with implications both for the fundamental understanding of the electronic, optical and magnetic properties and for the improvement of light-emitting efficiency of the material. In particular, recently it has been shown that enrichment of a-$Si_{1-x}C_x$:H films with carbon and low temperature annealing strongly enhance the intensity of the visible photoluminescence in this material.[11] However the origin of these phenomena is still unclear. At the same time the enrichment of a-$Si_{1-x}C_x$:H films with carbon correlated with the increase of the concentration of paramagnetic defects, among which the sp^3-coordinated silicon and carbon dangling bonds as well as sp^2-coordinated graphitelike carbon clusters are the most probable candidates.

The previous electron paramagnetic resonance (EPR) study of paramagnetic defects in near stochiometric and carbon-rich a-$Si_{1-x}C_x$:H films deposited by magnetron sputtering technique was performed at X-band frequency (9.4 GHz).[11,12] The EPR spectrum was represented by an isotropic single line with the g-value ($g=2.0026$) similar to that observed for a carbon related defect (CRD) in amorphous carbon.[13,14] Therefore the EPR signal with $g=2.0026$ was attributed to the CRDs. The EPR investigation was mainly focused on the analysis of the total concentration of paramagnetic defects and the width of the isotropic single line. But slight asymmetry of the X-band EPR signal of a-$Si_{1-x}C_x$:H films was reported in Ref. 12 and ascribed to the presence of silicon dangling bonds (SiDB) with $g=2.005$. The SiDB signal was also observed in optically detected magnetic resonance (ODMR) spectrum of a-$Si_{1-x}C_x$:H films with low content of carbon at $x\leq 5$ in.[3] The influence of hydrogen incorporation on paramagnetic response and characteristics of a-$Si_{1-x}C_x$:H thin films was discussed in Ref. 11. It was shown that annealing of the a-$Si_{1-x}C_x$:H films leads to the hydrogen effusion process in a-$Si_{1-x}C_x$:H films and causes an increase in the spin concentration of the CRD.

Recently high frequency (37 and 140 GHz) EPR study of carbon-rich a-$Si_{0.3}C_{0.7}$:H films showed that three EPR lines contribute to the isotropic line observed at X-band frequency.[15] The EPR lines were attributed to SiDBs, CRDs, and a bulk SiDB defect bonded with nitrogen atoms Si-N_2Si. The occurrence of the defect like Si-N_xSi_y is probably related to the residual nitrogen contamination of the films during the magnetron sputtering.

In this paper, we present the results of high-frequency (37 and 140 GHz) EPR study of the magnetic properties of the

SiDB and CRD in carbon-rich a-$Si_{0.3}C_{0.7}$:H films in the temperature interval from 4.2 to 300 K. It has been established that the temperature dependences of the integral intensities of the SiDB and CRD EPR signals do not obey the Curie-Weiss law, and the SiDB and CRD spin systems exhibit superparamagnetic and ferromagnetic properties, respectively.

The study of the impact of thermal annealing on the a-$Si_{0.3}C_{0.7}$:H films in the temperature range of T_{ann} =400–950 °C indicated that thermal annealing may be a desirable treatment depending on the property of interest. It was found that annealing treatment of the a-$Si_{0.3}C_{0.7}$:H films causes a beneficial effect of increasing the CRD density and can significantly alter the microstructure and magnetic properties of amorphous silicon carbide. In particular, the observed anisotropy of the g factor of CRD in high temperature annealed a-$Si_{0.3}C_{0.7}$:H films was explained by the formation of graphitelike sp^2-coordinated carbon nanoclusters and presence of the demagnetization field.

II. EXPERIMENTAL DETAILS

Amorphous hydrogenated silicon-carbon alloy films (a-$Si_{0.3}C_{0.7}$:H) were deposited by reactive dc-magnetron sputtering of a monocrystalline silicon target using a mixture of Ar/CH_4 as the working gas. Two-side polished Si (100) wafers (p type, 40 Ohm·cm) were used as the substrates. The substrate temperature during deposition was about 200 °C.

The details of the deposition procedure have been reported elsewhere.[12] The thickness of the a-$Si_{0.3}C_{0.7}$:H layer measured by interferometer was found to be 500 nm. The composition of the a-$Si_{1-x}C_x$:H was analyzed with Auger-electron spectroscopy JEOL Jump 10 s using relative sensitivity factors of core-valence lines of carbon (KVV) and silicon (LVV) obtained from the bulk 6H-SiC standard. Silicon-to-carbon ratio was estimated to be about 30/70.

After deposition, the samples were annealed in vacuum (10^{-6} Torr) for 15 min in the temperature range of 400–950 °C. Characterization of the surface morphology was performed by atomic force microscopy (AFM, Nanoscope IIIa) in the contact mode. The microstructure and the spatial distribution of carbon bonding states in the sample annealed at 950 °C were examined by high-resolution scanning transmission electron microscopy (STEM, Jeol-JEM200CX) equipped with electron energy loss spectrometer (EELS, Gatan ENFINA 1000).

EPR measurements at 37 GHz were performed using Bruker EMX spectrometer and a conventional Q-band EPR spectrometer equipped with a liquid helium cryosystem at temperatures between 4.2 and 300 K. EPR measurements at 140 GHz were performed using D-band EPR setup at 4.2 K. The error in g was estimated to be ± 0.0002. The magnetic fields were calibrated with the help of a Si:P (g=1.9985) standard sample. The spin densities were determined by a double integration of the experimental spectra and comparison with the Si:P spin standard sample. The estimated relative accuracy of the N_s measurements was $\pm 20\%$.

III. EXPERIMENTAL RESULTS

A. Atomic structure of the a-$Si_{0.3}C_{0.7}$:H film

The atomic structure of the a-$Si_{0.3}C_{0.7}$:H was investigated in as-deposited and annealed samples. Figure 1 shows a typical AFM image of the as-deposited a-$Si_{0.3}C_{0.7}$:H surface. One can readily observe the nano-meter-size surface morphology of the films. The surface profile, shown in Fig. 1, confirms and quantifies the nanostructured columnar morphology that is inherent to thin films deposited at low temperatures.[16] Large columns, 100–150 nm in diameter, are composed of thinner columns with diameters in the range of 20–40 nm.

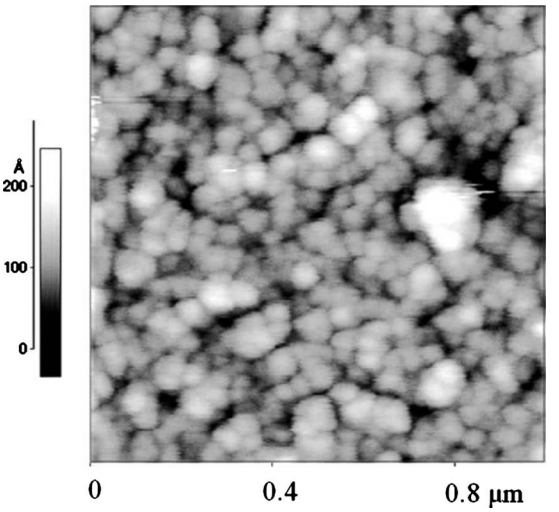

FIG. 1. AFM image of as-deposited a-$Si_{0.3}C_{0.7}$:H surface.

Elastic scattering STEM cross section image of a-$Si_{0.3}C_{0.7}$:H film annealed at 950 °C is shown in Fig. 2(a). The structure of the film is not homogeneous and contains nanoscale low-density regions (voids) elongated roughly perpendicular to the film surface and having a typical size of less than 5 nm in width and up to 50 nm in length. It is suggested that the observation of the voids in Fig. 2 is also an indication of columnar growth morphology.

The investigation of the spatial distribution of graphitelike carbon clusters was performed using energy filtered STEM

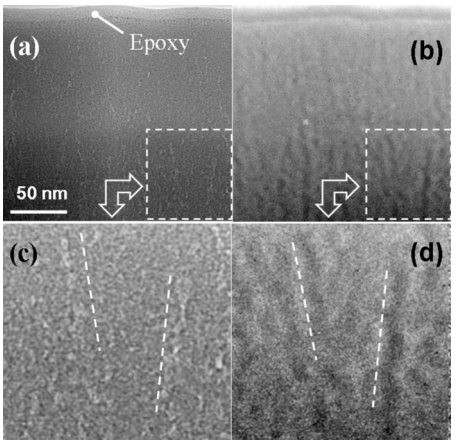

FIG. 2. STEM micrographs of an a-$Si_{0.3}C_{0.7}$:H sample annealed at 950 °C: a-Elastic scattering STEM cross-sectional image; b–STEM image based on EELS; c and d–higher magnification of the regions marked by the dashed lines in (a) and (b). Darker regions in (b) and (d) correspond to higher concentration of sp^2-coordinated carbon atoms.

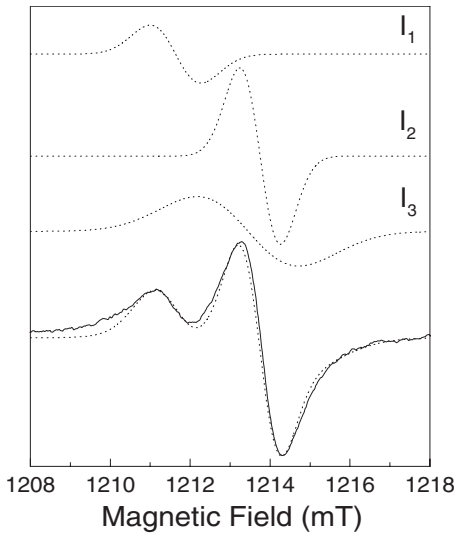

FIG. 3. Experimental and simulated Q-band EPR spectrum measured in as-deposited a-$Si_{0.3}C_{0.7}$:H films at 4.2 K. The solid line presents experimental data; the dashed lines are theoretical fits. Three dashed lines labeled I_1, I_2, and I_3 are fitted with Gaussian form.

measurements.[17,18] A narrow peak centered at 284 eV was observed in the electron energy loss spectrum of an a-$Si_{0.3}C_{0.7}$:H sample annealed at 950 °C. This peak is a fingerprint of graphite-like carbon and corresponds to the electron transition from the $1s$ to $2p_z$ unoccupied states ($1s \rightarrow \pi^*$) in the sp^2 hybrid orbital of carbon atom.[19,20] Figure 2(b) shows the map of the distribution of sp^2-coordinated carbon atoms generated by energy filtering of the electrons with energy loss around 284 eV. The darker regions correspond to higher concentration of sp^2-hybridized carbon atoms. The magnified images of the elastic scattering map and the sp^2-carbon bonding map are shown in Figs. 2(c) and 2(d), respectively. It is clearly seen that the spatial distribution of the graphitelike carbon is well correlated with the distribution of the nanovoids. Therefore, we can conclude that graphitic carbon that forms after the high-temperature annealing is predominantly localized in the nanovoids of the a-$Si_{0.3}C_{0.7}$:H film. It is well known that graphitelike clusters preferably condense on the surface in such a manner that graphene sheets form parallel to the surface.

B. General features of Q-band EPR spectrum in a-$Si_{0.3}C_{0.7}$:H film

Figure 3 shows experimental and simulated Q-band room temperature EPR spectrum obtained from as deposited a-$Si_{0.3}C_{0.7}$:H film. Deconvolution of the experimental EPR spectra was performed by using Easy-Spin-2.6.0 toolbox program.[21] The EPR spectrum of the as deposited a-$Si_{0.3}C_{0.7}$:H film is fitted with three Gaussian lines labeled I_1, I_2, and I_3. The I_1 line has a g-value of 2.0059(2) and the peak-to-peak linewidth $\Delta H_{pp}=1.2$ mT. These parameters identify this defect as a silicon (Si) dangling bonds (SiDBs) which is characterized by an isotropic g factor of 2.0055 ± 0.0005 and the linewidth of about (0.5–1.5 mT).[22] Somewhat higher g value of the I_1 line compared to that obtained for SiDB in amorphous Si ($g=2.0055$) at X-band frequency in[22] does not necessarily indicate a different nature of the EPR centers, but possibly points to the fact that chemical and structural surrounding of the SiDB in a-$Si_{0.3}C_{0.7}$:H film and a-Si:H are different.

The I_2 line is characterized by the isotropic g factor of 2.0028(2) and the peak-to-peak linewidth of $\Delta H_{pp}=1$ mT, which are the typical parameters for carbon-related defects (CRD) in amorphous carbon films.[14]

The third broad EPR signal had $g=2.0033(2)$ and the peak-to-peak linewidth of $\Delta H_{pp}=2.5 \pm 0.2$ mT. By comparing the g-value and the linewidth of the third EPR signal with the parameters of so-called K-centers previously observed in amorphous hydrogenated Si_3N_4 layers,[23] we may suggest that this EPR line is due to a defect similar to the K centers. The K centers are associated with threefold-coordinated SiDBs in which a Si atom could be bonded with one, two or three nitrogen atoms resulting to the formation of the ($Si\text{-}NSi_2$), ($Si\text{-}N_2Si$), and ($Si\text{-}N_3$) configurations, respectively. As a result, the g factor of the K center depends on the configuration of the defect and changes from 2.0030 to 2.0040, while the linewidth is mostly determined by unresolved superhyperfine interaction with ^{14}N ($I=1$) and ^{15}N ($I=1/2$) nuclei.[23] The obtained value of the g factor of 2.0033(3) demonstrated that the K center observed in a-$Si_{0.3}C_{0.7}$:H films has the $Si\text{-}N_2Si$ configuration. The occurrence of such defects in a-$Si_{0.3}C_{0.7}$:H films is probably related to the low-deposition temperature. Relative contribution of silicon- and carbon-related paramagnetic defects (N_{Si}/N_C) in as-deposited films was estimated to be about 1/5 with total concentration of spins of about $(5 \pm 0.1) \times 10^{19}$ cm^{-3}.

The effect of thermal annealing on the EPR spectrum of the a-$Si_{0.3}C_{0.7}$:H films was studied in the temperature range of $T_{ann}=400-950$ °C. As can be seen from Fig. 4, the amplitude of the CRD EPR signal increased by a factor of 40, while the integral intensity increased only by a factor of 8 due to the narrowing of the linewidth ΔH_{pp} at the annealing temperature of 950 °C.

The narrowing of the CRD EPR signal in the high temperature annealed a-$Si_{0.3}C_{0.7}$:H films is believed to be primarily due to spin-spin exchange interaction between charge carriers. The observed change in the linewidth was within the experimental error between 4.2 and 300 K ($\Delta H_{pp}=0.6 \pm 0.05$ mT), which excludes the possibility that the linewidth of the CRD EPR signal is determined by the motional narrowing effect, in which the linewidth becomes smaller at higher temperature. The suggestion that the exchange interaction occurs between charge carriers is consistent with the lineshape of the CRD signal being Lorentzian in high temperature annealed samples. It was found that EPR lineshape of the SiDB and CRD signals changes from a Gaussian for as-deposited sample to Lorentzian form in the sample annealed at 650 °C. The Gaussian line shape is expected when the linewidth is dominated by some unresolved hyperfine interaction. Therefore, the dominant contributions to ΔH_{pp} of SiDB and CRD signals should be attributed to unresolved hydrogen superhyperfine interaction in as deposited and low temperature annealed hydrogenated amorphous

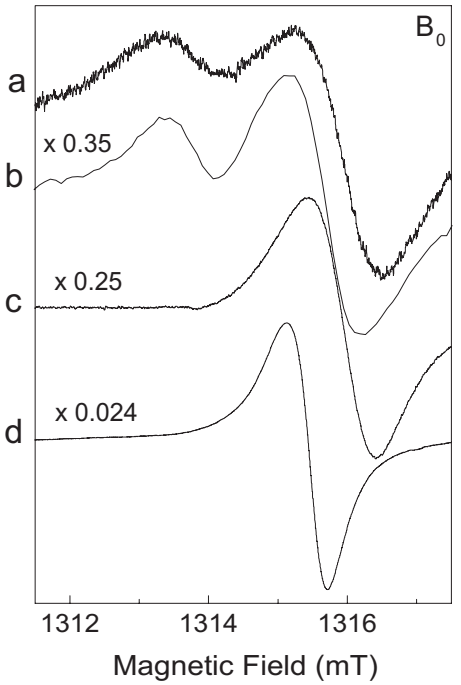

FIG. 4. *Q*-band EPR spectrum measured in as deposited and annealed a-$Si_{0.3}C_{0.7}$:H films at different amplification level. T =4.2 K. 1—as deposited; 2—T_{ann}=450 °C; 3—T_{ann}=650 °C: and 4—T_{ann}=950 °C.

(a-$Si_{0.3}C_{0.7}$:H) film. This conclusion is consistent with the temperature behavior of the EPR signal observed in as-deposited and low temperature annealed a-$Si_{0.3}C_{0.7}$:H films in[11] at *X*-band frequencies. The observed narrowing of the linewidth with increasing the temperature from 6 to 100 K was explained by thermally activated jumps of the unpaired electrons between hydrogen atoms. The change in the EPR lineshape from Gaussian to Lorentzian form after annealing the sample at 650 °C indicates that hydrogen effusion takes place at T_{ann} above 400 °C. Due to the hydrogen effusion process a strong increase in the concentration of the CRDs was observed in high temperature annealed a-$Si_{0.3}C_{0.7}$:H films. At the same time, as was shown in Fig. 4, EPR signal from Si-DB vanished upon annealing of a-$Si_{0.3}C_{0.7}$:H at T_{ann}=650 °C. The increase in the concentration of the CRDs indicates that carbon dangling bonds resulting from hydrogen release from the C-H bonds contribute to the CRD. Thus, the analysis of the integral intensity of the CRD signal, its line shape and width indicated that the exchange interaction between the spins of the CRDs occurs in the high temperature annealed samples. A similar behavior of the linewidth and line shape for CRD in high temperature annealed a-SiC:H films was observed by other authors[14,24] and was explained by formation of the sp^2 carbon clusters.

C. Anisotropy of the resonance magnetic field/*g*-factor of the CRD signal

For the a-$Si_{0.3}C_{0.7}$:H sample annealed at high temperature (950 °C) the temperature dependent resonance position/*g*-factor anisotropy was observed for CRD EPR signal when the orientation of the magnetic filed was varied relative to the film plane. The anisotropy of the resonance position of the CRD signal was found at *Q*-band and *D*-band frequencies, while at lower frequencies the anisotropy effect was hidden in the natural linewidth. As can be seen from Fig. 5, the orientation effect of the resonance field for the CRD signal was found to be higher at 140 GHz and 4.2 K with $B_{90} > B_0$, where B_0 and B_{90} correspond to the orientation of the magnetic field in-plane and normal to the film plane, respectively. The results of simulation of the CRD signal at 140 GHz indicated that the lineshape remains independent of the resonance microwave frequency and can be fitted with Lorentzian form, while the linewidth varies with orientation of the magnetic filed from 1 mT for B_{90} to 1.3 mT for B_0. This variation is due to the magnetic field scattering effect that occurs at high frequency and can be described by the ratio $\Delta\omega_{pp} = \gamma_e \Delta H_{pp}$,[25] where ω is the frequency of the microwave field; γ_e is the gyromagnetic ratio of the electron. The linewidth increases proportionally to the microwave frequency, which is due to a nonresolved dispersion of *g*-tensor components.

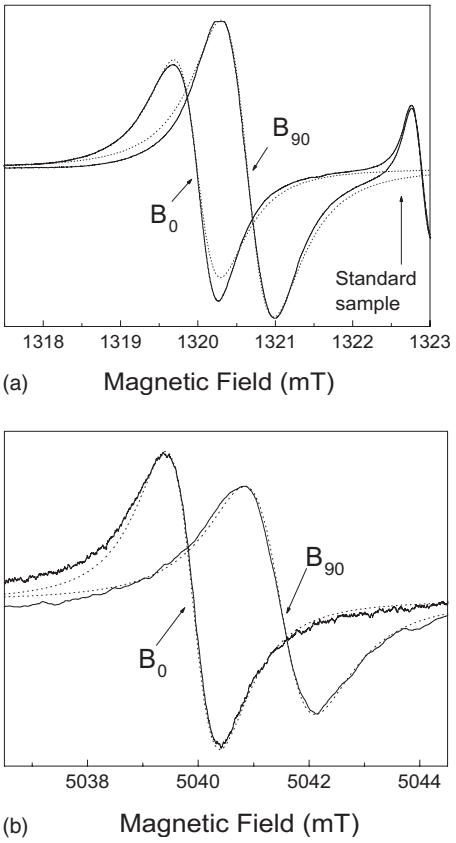

FIG. 5. Anisotropy of the resonance field of CRD EPR signal in a-$Si_{0.3}C_{0.7}$:H film annealed at T=950 °C at *Q*-band (a) and *D*-band (b) frequencies for variation of the magnetic field orientation from normal (B_{90}) to the film plane (B_0). T=4.2 K.

As follows from Fig. 6, the angular variation of the *g* factor of the CRD signal measured at 37 GHz in a-$Si_{0.3}C_{0.7}$:H sample annealed at high temperature (950 °C) may be fitted by the following expression:

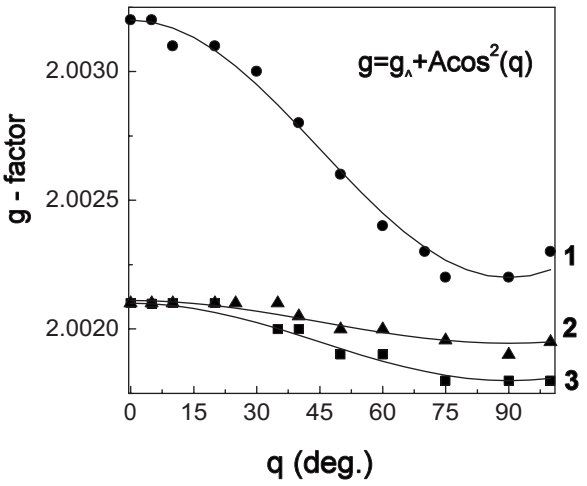

FIG. 6. The g-value anisotropy of the CRD spin resonance at different temperatures, measured in a-$Si_{0.3}C_{0.7}$:H sample annealed at 950 °C. The points are experimental data, the solid lines are the theoretical fits with Eq. (1): 1—4.2 K; 2—300 K; 3—77 K.

$$g = g_{\perp} + \mathrm{A} \cdot \cos^2 \theta, \tag{1}$$

where θ is the angle between the static magnetic field and the film plane, $\theta=0°$ corresponds to the magnetic field oriented in the film plane (B_0) and $\theta=90°$ is the case of the magnetic field normal to the film plane (B_{90}). The value of $g_{\perp}$ is independent of temperature and remains constant, whereas the anisotropy factor A is very strongly dependent on temperature and increases with decreasing temperature. It was found that $g_{\perp}=2.0023\pm0.0002$. The anisotropy A changes from 0.0002 at $T=300$ K to 0.0010 at $T=4.2$ K. From the fact that the g-value of the CRD signal exhibits the anisotropy we may conclude that the resonance arises from the unpaired spins located in the ordered phase of the film.

D. Temperature behavior of Q-band EPR spectra in a-$Si_{0.3}C_{0.7}$:H film

Figure 7 shows the temperature behavior of EPR spectra measured on samples annealed at 400 °C for the magnetic field orientation normal (B_{90}) to the a-$Si_{0.3}C_{0.7}$:H film plane. As can be seen from Fig. 7, the intensity of the EPR line of SiDB and CRD centers decreases with increasing the temperature. The temperature dependences of the integral intensities of CRD and SiDB resonance line observed in the sample annealed at 400 °C for the magnetic field orientation normal (B_{90}) and parallel (B_0) to the film plane is shown in Fig. 8. It is seen that they exhibit a different character of the temperature dependence, which is discussed in detail below. It should be noted that the temperature dependence of the intensities of the CRD and SiDB resonance lines was recorded at the same amplification level, and as a result the SiDB resonance line is hardly visible at $T=50$ K without gain variation.

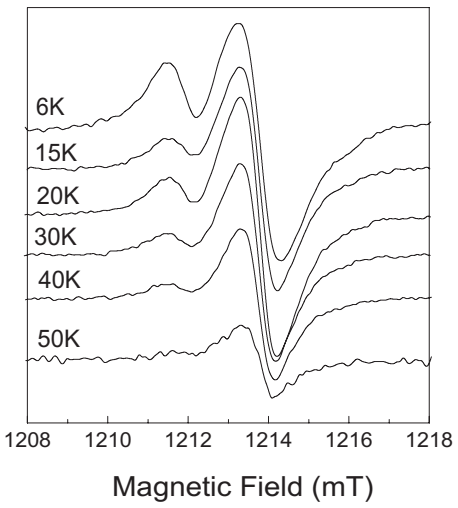

FIG. 7. Temperature behavior of the EPR spectrum measured on the a-$Si_{0.3}C_{0.7}$:H sample annealed at 400 °C with the magnetic field orientation normal to the film plane.

IV. ANALYSIS OF THE EXPERIMENTAL DATA AND DISCUSSION

A. Anisotropy of the resonance magnetic field of the CRD EPR signal

The anisotropy of the resonance position/g-factor observed for CRD EPR signal can serve as an evidence that a demagnetizing field exists in the a-$Si_{0.3}C_{0.7}$:H film. In contrast to the diluted paramagnetic materials, in which the demagnetizing fields are small relative to the linewidth the demagnetizing field becomes noticeable for the disordered materials such as amorphous layers in which the spins are coupled in clusters. These clusters can display ferromagnetic, antiferromagnetic or superparamagnetic behavior, which can be recognized by investigating the magnetization as function of applied magnetic field $M(B)$ at a given temperature and as a function of temperature $M(T)$ at a fixed field. The observation of the demagnetization effect in amorphous carbon at 9.4 GHz has been published earlier.[26] The influence of demagnetizing fields for a-C layers of about 10 mT was also observed at 285 GHz.[27]

Since the demagnetizing field B_{dem} is proportional to the magnetization M of the sample ($B_{\mathrm{dem}}=-4\pi M$), one can evaluate the sample magnetization M from the following expressions given in[28] for a thin layer:

$$(\omega/\gamma)^2 = B_0 \cdot (B_0 + 4\pi M),$$

$$(\omega/\gamma) = \mathrm{B}_{90} - 4\pi\mathrm{M}, \tag{2}$$

where ω is the frequency of the microwave field; $\gamma=\beta\cdot g_0$ is the gyromagnetic ratio of the spin system in the sample; β is the Bohr magneton, g_0 is the spectroscopic splitting factor g.

The Eq. (2) allow one to obtain two unknown values: $4\pi M$ and g_0. By combining these two equations one can obtain the sample magnetization value at two frequencies if the quadratic terms in Eq. (2) are neglected and the following experimental data are used: $B_{90}=1320.656$ mT and $B_0=1319.99$ mT at $\omega=37010.2$ MHz and $B_{90}=5043.14$ mT

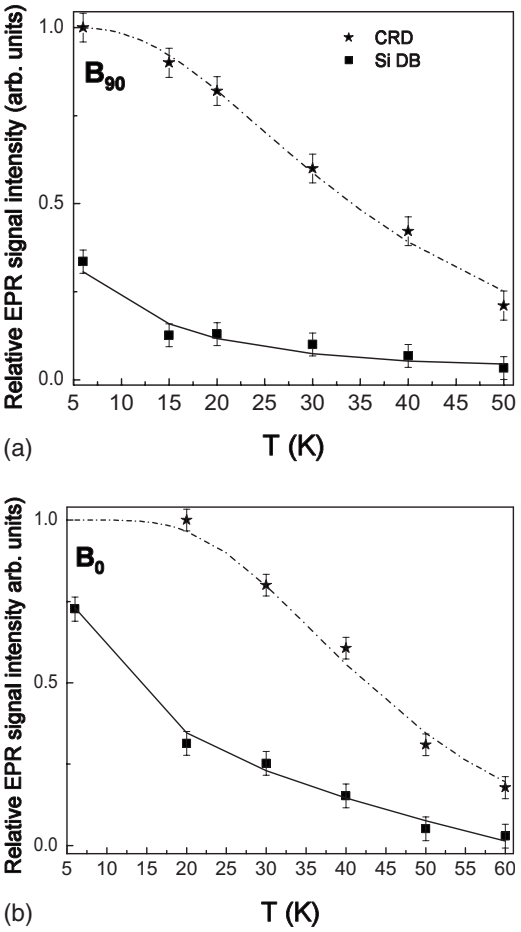

FIG. 8. The temperature dependences of the EPR signal intensity of the Si DB and CRD measured on the a-$Si_{0.3}C_{0.7}$:H sample annealed at 400 °C for the magnetic field orientation (a) normal (B_{90}) and (b) parallel (B_0) to the film plane. The points are experimental data, the solid and dash-dotted lines are theoretical fits with Eqs. (4) and (5), respectively.

and B_0=5041.49 mT at ω=141335.0 MHz. It was found that the magnetization field at 4.2 K in a-$Si_{0.3}C_{0.7}$:H film annealed at 950 °C is M=0.035 mT at 37 GHz and M =0.088 mT at 140 GHz.

The calculation of the gyromagnetic ratio of the spin system from the expression $g_0=\frac{3\cdot\omega}{\beta\cdot(2B_0+B_{90})}$ obtained from Eq. (2) yields g_0=2.0029 at 37 GHz and g_0=2.0028 at 140 GHz.

The spin concentration N_{CRD} estimated from the well-known expression for the paramagnetic susceptibilities $\chi = M/H = g_0^2\beta^2 N/(3\ kT)$ gives the concentration of the localized paramagnetic centers $N_{CRD}=9\times10^{19}$ cm^{-3}, while the estimation of the concentration of the spin system with ferromagnetic behavior from the relation $M_s=Ng_0\beta$ yields $N_{CRD}=5\times10^{19}$ cm^{-3}. The last value is comparable with the value of the total concentration of the spins found in as-deposited films, which was estimated to be of about $(5\pm0.1)\times10^{19}$ cm^{-3}. As was pointed out above, the relative accuracy of the N_s measurements was ±20%. Therefore it is most likely that the ferromagnetic rather than paramagnetic ordering in the spin system of the CRDs is responsible for the magnetization effect in a-$Si_{0.3}C_{0.7}$:H films. This conclusion is supported by the recently found ferromagnetism in carbon-based materials.[29]

On the other hand, the temperature dependent g-value anisotropy of the CRD signal observed in high temperature annealed samples correlates with that found previously for the charge carriers in monocrystalline graphite, but the anisotropy value A for CRD signal is smaller. The observed value A for pure graphite at 300 K is A=0.047 and A =0.125 at T=4.2 K,[30] while for CRD in a-$Si_{0.3}C_{0.7}$:H film A=0.0002 at T=300 K and A=0.0010 at T=4.2 K.

The g-value anisotropy for the charge carriers was also observed in polycrystalline and nanocrystalline graphite and in amorphous carbon a-C:H. In these materials g tensor of the charge carriers have the same g value in the sheet plane ($B\perp c$) of $g_\perp=2.0028\pm0.0002$ and varies as magnetic filed is normal ($B\|c$) to the sheet plane from $g_\|=2.0182$ for polycrystalline graphite to $g_\|=2.005$ for nanocrystalline graphite and amorphous carbon at 4.2 K. It was found that the magnitude of the anisotropy A depends strongly on the graphite particle size and has the smallest value for the nanosized graphitic sp^2 clusters formed in amorphous carbon.[31] Considering that the anisotropy factor A (0.0022) and spin concentrations (10^{19}–10^{21} cm^{-3}) in a-C:H had values close to the ones observed in this study, we can conclude that the anisotropy of the CRD signal originates from graphitelike sp^2-bonded carbon nanoclusters that are formed in the high temperature annealed a-$Si_{0.3}C_{0.7}$:H film. In accordance with the relationship between the numerical value of $g_\|$ and the sp^2 cluster size found for amorphous carbon in,[31] the size value of sp^2 graphitelike clusters formed in a-$Si_{0.3}C_{0.7}$:H film was estimated to be below 5 nm. This result is in agreement with the nanometer size of the sp^2 carbon clusters (1.2–2.5 nm) deduced from the Raman measurements in the high temperature annealed a-SiC:H films.[10] Taking into account the porous columnar morphology of the a-$Si_{0.3}C_{0.7}$:H film [Fig. 1 and 2(a)], and the map of distribution of sp^2-coordinated carbon atoms obtained by energy filtered STEM measurements, shown in Fig. 2(b), it is expected that the graphitization occurs at the column surface oriented perpendicular to the film plane. This conclusion is justified by the fact that the electrical conductivity of a-$Si_{0.3}C_{0.7}$:H in the film plane is a several times smaller than the conductivity normal to the film plane. Indeed, as was shown in,[30] the conductivity of graphite along the c axis is 100 to 200 times smaller than that in the film plane. Thus, the direction of the conductivity anisotropy in a-$Si_{0.3}C_{0.7}$:H agrees with that in graphite if one assumes that the graphitization occurs along the columns, and as a result the c axis of the graphitic layer is oriented roughly along the film plane.

Comparison of the anisotropy behavior of the g-value in a-$Si_{0.3}C_{0.7}$:H with that in graphite also confirms this conclusion. The angular dependence of the g-factor for a-$Si_{0.3}C_{0.7}$:H correlates with that for graphite if the direction normal and parallel to the crystallographic c axis[30] in graphite corresponds to the θ=0° and θ=90° in a-$Si_{0.3}C_{0.7}$:H, respectively.

Thus, the observed g-value anisotropy of the CRD signal is caused by the presence of the sp^2-coordinated carbon clusters and by the presence of a demagnetization field (shape-dependent anisotropy term) the magnitude of which depends

on the value of the applied external magnetic field. But it remains unclear how to distinguish between these two contributions that caused the observed g-value anisotropy of the CRD signal.

Considering that the material comprises a mixture of the sp^2 and sp^3 carbons, we could make an attempt to evaluate the contribution of the graphitelike sp^2 fraction in respect to the sp^3 carbon matrix in as deposited a-$Si_{0.3}C_{0.7}$:H using the relation for the effective magnetic resonance field of two paramagnetic subsystems coupled by exchange interaction:[32]

$$B_{\mathrm{res}} = \frac{\chi_1 B_{\mathrm{res},1} + \chi_2 B_{\mathrm{res},2}}{\chi_1 + \chi_2} \tag{3}$$

where $\chi_{1,2}$ are the magnetic susceptibilities of the two spin subsystems. One of them belongs to the carbon dangling bonds with isotropic $g=2.0028$, the second one belongs to the charge carriers in graphite with the maximum value of the g-factor $g=2.0496$ at $T=300$ K. B_{res} is the observed resonance magnetic field, $B_{\mathrm{res},1}$ and $B_{\mathrm{res},2}$ are the resonance magnetic fields for the individual subsystems in the absence of the exchange interaction.

The susceptibilities ratio χ_1/χ_2, i.e., the ratio between the spin concentrations of the two subsystems, may be calculated by using the expression (3). It was found that the concentration of the graphitelike sp^2 dangling bonds amounts to 1.1% of the total concentration of the carbon dangling bonds in as deposited a-$Si_{0.3}C_{0.7}$:H.

B. Magnetic properties of the SiDB and CRD

The information about magnetic state of the spin system responsible for the observed magnetic properties of a-$Si_{0.3}C_{0.7}$:H film can be also derived from the temperature dependence of the integral intensities of the SiDB and CRD EPR signals shown in Fig. 8. In principle one can expect that three types of magnetic systems could be presented in disordered material such as a-$Si_{1-x}C_x$:H films: (1) a paramagnetic system of the uncoupled spins with the Curie-Weiss temperature behavior of magnetic susceptibility χ(T), (2) a system of superparamagnetic clusters in which unpaired spins are coupled to a quite large magnetic moments, and (3) a system of spin clusters with ferromagnetic coupling occurred in disordered range. Analysis of the temperature dependences of the integral intensities of the SiDB and CRD EPR signals has shown that they do not obey the Curie-Weiss law, and their spin systems exhibit superparamagnetic and ferromagnetic properties, respectively.

Superparamagnetism is normally found for the superspins coupled to the clusters with the large magnetic moments. These superspins behave such as individual spins in paramagnetic materials and as a result their temperature properties are described by the Langevin function $L=\coth(\theta/T)-T/\theta$, where $\theta=\frac{\mu_B \cdot H \cdot n}{k}$, k—Boltzmann constant, H—resonance magnetic field value; n—the number of spins in the cluster; θ—is the energy of the total magnetic moment $(n \cdot \mu_B)$ in the presence of the magnetic field H. θ is given in the temperature units; μ_B is the Bohr magneton.

In the real system with the high concentration of paramagnetic centers, the number of the spins in the clusters may vary in a wide range. As a consequence, assuming that the clusters have a size distribution, the temperature dependence of the integral intensity of the SiDB resonance line was fitted with the integral of the Langevin function

$$I(T) = A \cdot T \cdot \int_{\theta_1/T}^{\theta_2/T} \left[\coth\left(\frac{\theta}{T}\right) - \frac{T}{\theta} \right] d\left(\frac{\theta}{T}\right) = A \cdot T \cdot \ln\left[\frac{\sinh\left(\frac{\theta_2}{T}\right)}{\left(\frac{\theta_2}{\theta_1}\right) \cdot \sinh\left(\frac{\theta_1}{T}\right)} \right]. \tag{4}$$

The θ_1 and θ_2 are the integration limits corresponding to the minimum and the maximum number of spins in the clusters, respectively.

By fitting the temperature curve in Fig. 8 with Eq. (4) it was found that the spin number in Si clusters varies from $n_{\min}=16$ to $n_{\max}=25$, for the magnetic field orientation parallel to the film plane and from $n_{\min}=20$ to $n_{\max}=32$ for the magnetic field orientation normal to the film plane. The fact that the temperature dependence of the signal intensity of Si DB resonance line is described by the Langevin function indicates that the SiDB clusters exhibit superparamagnetic behavior.

Unlike the temperature curve of the SiDB resonance line, the temperature curve of the CRD signal intensity, shown in Fig. 8, is concaved. As can be seen from Fig. 8, down to below 20 K the CRD signal intensity reaches its constant value, which is caused by saturation of the magnetization at low temperature. The temperature dependence of the CRD EPR signal intensity correlates with the temperature behavior of magnetization curves observed for the clusters with ferromagnetic ordering in a disordered system, which was described by percolation mechanism of free-charge carriers across the clusters.[33] Due to the ferromagnetic exchange interaction between spins through the random jumps of free charge carriers, the spin clusters are coupled into the bulk total magnetic moment. According to the model of magnetization in a disordered system the temperature dependence of the CRD signal intensity is described by the expression:[33]

$$I(T) = I_0 \cdot \left\{ 1 - \exp\left[-\nu_R \cdot \ln^3\left(\frac{J_0}{T}\right) \right] \right\}, \tag{5}$$

where $\nu_R = \frac{4}{3}\pi \times n \times R^3$; n is the spin number in the unit of the volume, R is an effective radius of the exchange interaction between spins; J_0 energy of the exchange interaction between the nearest spins.

The fitting of the theoretical function (5) to the experimental temperature curve in Fig. 8 allows one to obtain the energy of the exchange interaction J_0 between the nearest spins for CRD. It was found that $J_0=13.3$ meV for the magnetic field orientation parallel to the film plane and $J_0=10.7$ meV for the magnetic field orientation normal to the film plane. The ν_R value is 0.55 and 0.2 for the magnetic field orientation parallel and normal to the film plane, respectively.

The obtained results are in agreement with the main principle formulated for the carbon based materials in Ref. 34

stating that all constituent atoms and molecules should be paramagnetic and interaction should be ferromagnetic. Particularly, the two sp^2 carbon radicals separated by a carbon atom in sp^3 state interact ferromagnetically. In the case of a-$Si_{0.3}C_{0.7}$:H films a coexistence of ferromagnetic and paramagnetic spins is suggested, which is supported by the fact that 1.1% of the ferromagnetic sp^2-bonded carbon nanoclusters are dispersed in a sea of the paramagnetic spins with isotropic $g=2.0028$.

V. CONCLUSIONS

High-frequency EPR study of as deposited hydrogenated carbon-rich silicon-carbon alloy (a-$Si_{0.3}C_{0.7}$:H) films in the temperature interval from 4.2 to 300 K have shown that the EPR spectrum of a-$Si_{0.3}C_{0.7}$:H consists of three lines with $g=2.0059$, $g=2.0028$ and $g=2.0033$. The first two of those lines were assigned to SiDB and sp^3-coordinated hydrocarbon related paramagnetic defects (CRD), respectively. The g-value and the linewidth obtained for the third EPR signal are similar to the corresponding parameters of the so-called K center observed in amorphous hydrogenated Si_3N_4 layers and having Si-N_2Si configuration.[23] Therefore it was suggested that the third EPR line with $g=2.0033$ represents the threefold-coordinated SiDBs in which a Si atom is bonded with two nitrogen N atoms (Si-N_2Si).

The effect of thermal annealing on the EPR spectrum of the a-$Si_{0.3}C_{0.7}$:H films was studied in the temperature range of $T_{ann}=400-950$ °C. The analysis of the line shape and linewidth of the CRD and SiDB signals in as-deposited and annealed a-$Si_{0.3}C_{0.7}$:H films showed that the dominant contributions to the linewidth (ΔH_{pp}) of SiDB and CRD signals in as-deposited and low temperature annealed a-$Si_{0.3}C_{0.7}$:H films is due to unresolved hydrogen super-hyperfine interaction. It was established that hydrogen effusion process occurred in a-$Si_{0.3}C_{0.7}$:H at T_{ann} above 400 °C. Hydrogen loss from C-H bonds starts at 450 °C and leads to the strong increase in the concentration of the CRDs. The increase in the concentration of the CRDs is accompanied by the exchange narrowing of their EPR linewidth. The g-factor of the CRD signal in a-$Si_{0.3}C_{0.7}$:H sample annealed at high temperature (950 °C) shows, similar to the case of charge carriers in graphite materials, a strong anisotropy, which magnitude is temperature dependent and increases with decreasing the temperature. The similarity in the behavior of the g-factor anisotropy for the charge carriers in graphitelike materials and in amorphous SiC indicates that the graphitelike sp^2-bonded carbon clusters are formed in the high temperature annealed a-$Si_{0.3}C_{0.7}$:H.

Taking into account the porous columnar morphology observed in as deposited a-$Si_{0.3}C_{0.7}$:H film and the particular pattern of the spatial distribution of graphitelike carbon clusters in high temperature annealed a-$Si_{0.3}C_{0.7}$:H obtained with a STEM based on EELS, it was concluded that the graphitization occurs at the column surface and is oriented roughly perpendicular to the film plane. This conclusion is in agreement with the observed anisotropy of the resonance magnetic field of the CRD defect and anisotropy of the conductivity observed in high temperature annealed a-$Si_{0.3}C_{0.7}$:H samples.

On the other hand, the anisotropy of the g-factor observed for the CRD signal at Q-band and D-band frequencies is explained by the influence of demagnetizing fields, which is becoming significant at high-spin density of the paramagnetic centers, higher microwave frequency, and low temperature. It was found that the demagnetizing field which is proportional to the magnetization of the sample M is equal to 0.035 mT at 37 GHz 0.088 mT at 140 GHz.

The information about the magnetic state of the spin system responsible for the observed magnetic properties of a-$Si_{0.3}C_{0.7}$:H film was obtained from the temperature dependence of the integral intensities of the SiDB and CRD EPR signals. The fact that the temperature dependence of the signal intensity of the SiDB resonance line is described by the Langevin function indicates that SiDB clusters exhibit superparamagnetic behavior. It was found that the spin number in the Si clusters varies from $n_{min}=16$ to $n_{max}=25$, for the magnetic field orientation parallel to the film plane and from $n_{min=}20$ to $n_{max}=32$ for the magnetic field orientation normal to the film plane.

It was found that the temperature dependence of CRD EPR signal intensity correlates with the temperature behavior of the magnetization curves observed for the clusters with ferromagnetic ordering in disordered system. Due to the exchange interaction between the free-charge carriers the spin clusters are coupled into the bulk total magnetic moment exhibiting the ferromagnetic behavior.

ACKNOWLEDGMENT

The work was partially supported by Civilian Research & Development Foundation (Project No. UKE2-2856).

[1] J. Bullot and M. P. Schmidt, Phys. Status Solidi B **143**, 345 (1987).
[2] R. S. Sussmann and R. Ogden, Philos. Mag. B **44**, 137 (1981).
[3] S. Liedtke, K. Lips, M. Bort, K. Jahn, and W. Fuhs, J. Non-Cryst. Solids **114**, 522 (1989).
[4] T. Ma, J. Xu, K. Chen, J. Du, W. Li, and X. Huang, Appl. Phys. Lett. **72**, 13 (1998).
[5] J. Niemann and W. Bauhofer, Thin Solid Films **352**, 249 (1999).
[6] L. Magafas and J. Kalomiros, Microelectron. J. **38**, 1196 (2007).
[7] L. F. Marsal, I. Martin, and J. Pallares, J. Appl. Phys. **94**, 2622 (2003).
[8] D. Kruangam, F. Wongwan, T. Chutarasok, K. Chirakawikul, and S. Panyakeow, J. Non-Cryst. Solids **266-269**, 1241 (2000).
[9] S. F. Cogan, D. J. Edell, A. A. Guzelian, Y. Ping Lin, and R. Edell, J. Biomed. Mater. Res. Part A **67A**, 856 (2003).
[10] J. M. Hsu, P. Tathireddy, L. Rieth, A. R. Normann, and F. Solzhacher, Thin Solid Films **516**, 34 (2007).
[11] A. V. Vasin, S. P. Kolesnik, A. A. Konchits, A. V. Rusavsky, V.

S. Lysenko, A. N. Nazarov, Y. Ishikawa, and Y. Koshka, J. Appl. Phys. **103**, 123710 (2008).
[12] A. V. Vasin, S. P. Kolesnik, A. A. Konchits, V. I. Kushnirenko, V. S. Lysenko, A. N. Nazarov, A. V. Rusavsky, and S. Ashok, J. Appl. Phys. **99**, 113520 (2006).
[13] J. Robertson, Phys. Status Solidi A **186**, 177 (2001).
[14] F. Giorgis, A. Tagliaferro, and M. Fanciulli, *Amorphous Carbon: State of the Art*, Proceedings of the 1st International Specialist Meeting on Amorphous Carbon-SMAC '97 Amorphous Carbon, edited by S. R. Silva, J. Robertson, W. I. Milne, and G. A. J. Amaratunga (World Scientific, Singapore, 1998).
[15] A. V. Vasin, E. N. Kalabuhova, S. N. Lukin, D. V. Savchenko, V. S. Lysenko, A. N. Nazarov, A. V. Rusavsky, and Y. Koshka, Mater. Res. Soc. Symp. Proc. **1069**, 175 (2008).
[16] R. Messier, A. P. Giri, and R. A. Roy, J. Vac. Sci. Technol. A **2**, 500 (1984).
[17] R. F. Egerton, *Electron Energy-Loss Spectroscopy in the Electron Microscope* (Plenum Press, New York, 1996).
[18] W. Grogger, M. Varela, R. Ristau, B. Schaffer, F. Hofer, and K. M. Krishnan, J. Electron Spectrosc. Relat. Phenom. **143**, 139 (2005).
[19] *Transmission Electron Energy Loss Spectrometry in Materials Science and the EELS ATLAS*, edited by Channing C. Ahn (Wiley-VHC, New York, 2004).
[20] S. Muto, A. V. Vasin, Y. Ishikawa, N. Shibata, J. Salonen, and V.-P. Lehto, Mater. Sci. Forum **561-565**, 1127 (2007).
[21] S. Stoll and A. Schweiger, J. Magn. Reson. **178**, 42 (2006).
[22] M. H. Brodsky and R. S. Title, Phys. Rev. Lett. **23**, 581 (1969).
[23] P. Aubert, H. J. von Bardeleben, F. Delmotte, J. L. Cantin, and M. C. Hugon, Phys. Rev. B **59**, 10677 (1999).
[24] T. Christidis, M. Tabbal, S. Isber, M. A. El Khakani, and M. Chaker, Appl. Surf. Sci. **184**, 268 (2001).
[25] J. H. Freed, in *Very high frequency (VHF) ESR/EPR*, edited by O. Y. Grinberg and L. J. Berliner (Kluwer Academic/Plenum Publishers, New York, 2004), Chap. 2, p. 22.
[26] B. Druz, I. Zaritskiy, Y. Yevtukhov, A. Konchits, M. Valakh, S. Kolesnik, B. Shanina, and V. Visotski, Mater. Res. Soc. Symp. Proc. **593**, 249 (2000).
[27] H. J. von Bardeleben, J. L. Cantin, K. Zellama, and A. Zeinert, Diamond Relat. Mater. **12**, 124 (2003).
[28] C. Kittel, *Introduction to Solid State Physics*, 4th ed. (Wiley, New York, 1976).
[29] J. Cervenka, M. I. Katsnelson, and C. F. J. Flipse, Nat. Phys. **5**, 840 (2009).
[30] G. Wagoner, Phys. Rev. **118**, 647 (1960).
[31] H. J. von Bardeleben, J. L. Cantin, A. Zeinert, B. Racine, K. Zellama, and P. N. Hai, Appl. Phys. Lett. **78**, 2843 (2001).
[32] J. Winter, *Magnetic Resonance in Metals* (Clarendon Press, Oxford, 1971), Chap. 10, p. 256.
[33] Ya. Korenblit and E. F. Schender, Sov. Phys. Usp. **21**, 832 (1978).
[34] T. L. Makarova, Semiconductors **38**, 615 (2004).